Available online at www.sciencedirect.com
ScienceDirect
Journal of Hazardous Materials 156 (2008) 356–364
Journal of Hazardous Materials
www.elsevier.com/locate/jhazmat

Feasibility of destruction of gaseous benzene with dielectric barrier discharge

Zhaolian Ye [a,b], Yaning Zhang [a], Ping Li [a], Longyu Yang [a], Renxi Zhang [a,*], Huiqi Hou [a,*]

[a] *Institute of Environmental Science, Fudan University, Shanghai 200433, PR China*
[b] *Jiangsu Teacher's University of Technology, Changzhou 213001, PR China*

Received 12 September 2007; received in revised form 3 December 2007; accepted 10 December 2007
Available online 23 December 2007

Abstract

Destruction of gaseous benzene (C_6H_6) by dielectric barrier discharge (DBD) was studied in both laboratory-scale and scale-up DBD systems. The effects of input power, gas flow rate as well as initial concentration on benzene decomposition and energy yield were investigated. In addition, qualitative analysis on byproducts and relatively detailed discussion on mechanisms were also presented in this paper. At last, we systematically illustrated the feasibility of benzene removal with DBD on basis of three aspects: estimation of treatment cost per unit volume, comparison with other plasmas, and problems existed in DBD system. The results will help impel actual application of DBD on waste gas containing benzene.

Keywords: Benzene destruction; Dielectric barrier discharge; Feasibility; Mechanism

1. Introduction

Benzene is one of the important volatile organic compounds (VOCs) and widely used as petrifaction material in many industrial applications such as dope, paints, chemical plants, and printing industries. C_6H_6 has high toxicity and breathing C_6H_6 can cause drowsiness, dizziness, and unconsciousness. Moreover, repeated exposure can have adverse impacts on human health including anemia, leukemia, blood diseases, and cancer.

Up to now, it is still a hard work to treat industrial C_6H_6 waste gas due to the special stability of C_6H_6 and the inaccessibility of conventional techniques. In recent years, there have been many reports [1,2] on dielectric barrier discharge (DBD) used for treating pollutants as an alternative approach. As reported, DBD can be used to decompose most of VOCs, such as benzene [3–6], toluene [7,8], xylene [9] and styrene [10,11]. However, in their studies, pollutants were removed under static state or low-flow case (gas flow rate = 0.1–1 L/min), which was varied to effluent rate of typical industrial exhausts. There have little reports on waste gas treatment under high-flow rate with DBD, which is considered probably more close to practical exhausts treatment. The more important thing is that we have not found any systematic investigation on the feasibility of C_6H_6 removal with DBD. So far, there have only been two reports on practical industrial waste gas removal with DBD. One is dioxins removal with DBD by Fujistu Company. The investigation [12] shows that removal efficiency can reach 90% for 1 $\mu g/m^3$ dioxins. The other case [13] is that DBD designed by our institute was successfully applied for decomposing industrial waste gas containing sulfured hydrogen (H_2S) and carbon disulfide (CS_2) from YueJi Chemical Fiber Company in Shanghai. The system has run properly 8 years with removal efficiencies of H_2S and CS_2 of 85% and 86.5%. For promoting industrial applications, one very important issue is how to scale up plasma reactor in order to achieve maximum removal efficiency at minimal cost. Thus, we think it is very essential to study removal feasibility of benzene with DBD on basis of scale-up experiment and cost estimation and so on.

The aim of this paper is to illustrate systematically the feasibility of C_6H_6 removal with DBD on basis of four aspects: removal efficiency and energy yield analysis versus parameters, scale-up experiment study, byproducts and mechanism analysis, and feasibility study. We made attempt to provide relative all-

* Corresponding authors. Tel.: +86 21 6564 2293; fax: +86 21 6564 3849.
E-mail address: fdesi@fudan.edu.cn (R. Zhang).

0304-3894/$ – see front matter © 2007 Elsevier B.V. All rights reserved.
doi:10.1016/j.jhazmat.2007.12.048

Nomenclature

C_{in}	initial benzene concentrations (mg/m^3)
DBD	dielectric barrier discharge
Ey	energy yield (g/kWh)
k_E	energy constant (L/J)
Md	mineralization degree (%)
P	input power (W)
Q	gas flow rate (m^3/h)
Rh	relative humidity (%)
S_{CO_2}	selectivity of CO_2 (%)
SED	specific energy density (J/L)
T	surrounding temperature (K)
TCP	treatment cost per unit volume ($/kWh)

Greek letter

η, $\eta_{benzene}$	removal efficiency of benzene (%)

around analysis to C_6H_6 destruction in DBD, which will give some valuable proposals to commercial availability.

2. Experimental

2.1. Laboratory-scale DBD system

Fig. 1 shows the laboratory-scale DBD system which consists of a self-designed continuous flow gas generation system, a laboratory-scale DBD reactor, and a gas detection system. In numerous studies [6,14], gaseous C_6H_6 was produced by bubbling liquid C_6H_6 to form saturated vapor, which was then mixed with compressed air in a buffer bottle to form gaseous C_6H_6 with certain concentration. In this study, we designed a gas generation system with simple operation. The gas from compressed air cylinder flowed through six bottles filled with liquid C_6H_6, carrying gaseous C_6H_6 on liquid surface, and then mixed and diluted with surrounding air in a mixing chamber to form gaseous C_6H_6 with certain concentration which was fed axially into the DBD reactor under a tunable air blower (pressure loss is 1000 Pa). Thus, the pressure in discharge zone is lower than atmospheric pressure but near atmospheric pressure. By means of an exhaust fan (2X-3, China) connected with six-way-valve autosampler, samples, before and after discharge reaction, could be taken from the plasma reactor exit and analyzed by an on-line gas chromatograph (GC-930, China). To make sure discharge arrived at steady state, the gaseous sample for analysis was taken at a time around 30 min after discharge started. Noticeably, since the system is an open system, surrounding temperature and humidity is variable due to weather condition. Nevertheless, contrast experiment was conducted at constant surrounding temperature (T) and relative humidity (Rh) to ensure the accuracy of the results.

The DBD reactor was made of two coaxial quartz tubes with wall thickness of 2.0 mm and length of 200 mm. The inner one had an outside diameter of 10 mm, while the outer one had an inside diameter of 26 mm. A stainless foil attached tightly to the inside wall of the inner tube serving as an inner electrode. The outer electrode, made of a stainless strip with a width of 4 mm, was wrapped around the outside of the external tube with 4 mm spacing. The discharge region was sustained within a constant volume of 63.3 mL. A homemade square wave high-voltage supply with a fixed frequency of 20 kHz was used for generating plasma discharge with peak voltage ranging from 3 to 9 kV measured by a high voltage probe (XJ 2370, China). In this research, it was assumed that the power consumed in the circuit could be neglected. This meant that the energy provided by power supply was equal to the energy acted on the two electrodes of DBD. The current can be observed on the relative instrument panel. Detailed measurement of the discharge power has been previously reported by our group [15,16].

2.2. Scale-up DBD system

To simulate practical exhausts of benzene, characterized as low-concentration and high-flow rate, we designed our scale-up DBD reactor in terms of parallel connection with 10 discharge tubes. Each discharge tube was connected with an alone high voltage power supply and had the same dimensions (inner diameter of outer tube: 40 mm; outer diameter of inner tube: 10 mm; length: 300 mm; wall thickness: 2 mm), resulting in total gas flow rate is 509 m^3/h. Gas stream containing C_6H_6 first passed through gas/water separator to get rid of water in gas streams, followed by baffle mixture, and then was fed axially into each discharge tube. The clean gas exhausted by chimney. The detailed schematics are plotted in Fig. 2.

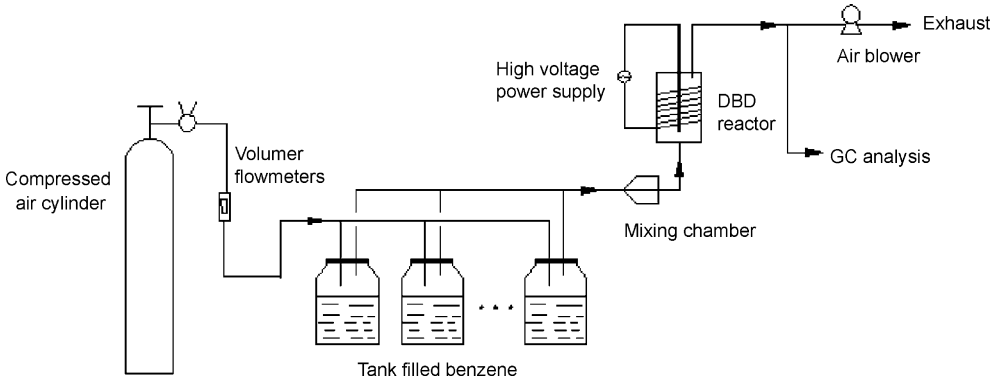

Fig. 1. Schematics of laboratory-scale DBD system.

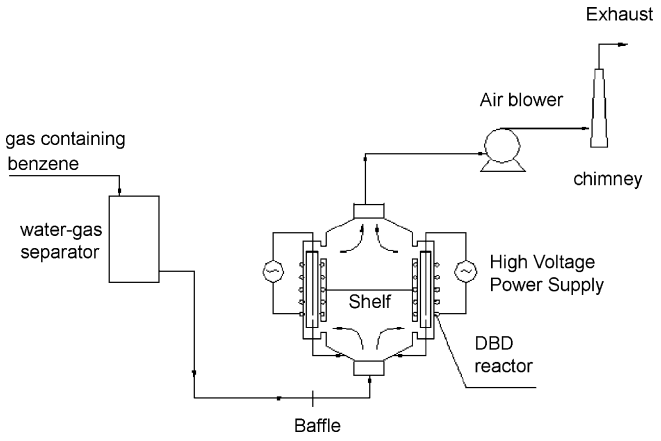

Fig. 2. Schematics of the scale-up DBD system.

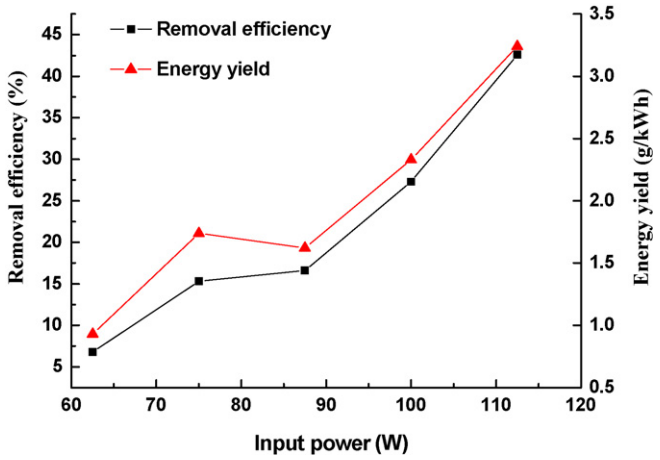

Fig. 3. Effect of input power on $\eta_{benzene}$ and Ey (T = 289K, Rh = 70%, Q = 2.44 m^3/h, C_{in} = 350 mg/m^3).

2.3. Analysis methods

Unreacted gaseous samples were analyzed by gas chromatograph (GC-930, China) with a 2-m long Porapak Q column maintained at 473 K and a hydrogen flame ionization detector (FID). Removal efficiency of benzene ($\eta_{benzene} = (C_{in} - C_{out})/C_{in}$, C_{in} and C_{out} are the inlet and the outlet concentration of C_6H_6, mg/m^3) was calculated from the GC peak areas before and after discharge. Carbon monoxide (CO) and carbon dioxide (CO_2) were separated with a 1-m long Molecular Sieve TXM column maintained at 343 K. Mineralization degree ($Md = (1000[CO_2] + [CO])M/6C_{in}\eta_{benzene}$; $[CO_2]$ and [CO] are the concentration of CO_2 and CO produced in discharge (mol/m^3); M is molecular weight of C_6H_6, g/mol) and CO_2 selectivity ($S_{CO_2} = [CO_2]/([CO_2] + [CO])$) are proposed to describe the degree of complete degradation and byproducts safety.

Solid depositions on the internal wall of DBD reactor were collected and analyzed by a Fourier transformation infrared spectrometer (FT-IR, Avatar-360, America) and a gas chromatography-mass spectrometry (GC-MS, HP 5973-6890, America). Aerosol particles existed in effluent were collected by portable particles sizer (Dust-Sol, China).

As a measure of the energy efficiency, energy yield ($Ey = QC_{in}\eta_{benzene}/P$ (g/kWh); Q denotes gas flow rate (m^3/h); P is input power (W)) was used.

3. Results and discussions

3.1. Study of benzene removal in laboratory-scale DBD

3.1.1. Influence factors of C_6H_6 destruction

Fig. 3 shows the relationship between $\eta_{benzene}$ and Ey and input power. The experimental conditions are: C_{in} of 350 mg/m^3, Q of 2.44 m^3/h, T of 289 K and Rh of 70%. From Fig. 3, both $\eta_{benzene}$ and Ey increase quickly with increasing input power.

It is well known that gas flow rate has a significant impact on pollutant decomposition via changing the residence time in DBD. As shown in Fig. 4, with Q increasing from 0.6 to 5.4 m^3/h, $\eta_{benzene}$ drops quickly from 100 to 13.5%, which can be explained that residence time correspondingly reducing with the rise of Q for a changeless reactor volume leads to the decrease in colliding frequency of electrons with gaseous C_6H_6 molecule per unit. On the other hand, Ey increases from 3.91 to 9.45 g/kWh when Q rises from 0.6 to 2.1 m^3/h, but starts to decrease as Q further increases. Thus, we concluded that the value of Q is crucial to gain advisable removal efficiency and energy yield. The results in Fig. 4 were achieved at input power of 135 W, C_{in} of 880 mg/m^3, T of 289 K and Rh of 42%.

Generally speaking, concentration of actual industrial exhausts varies at intervals, so it is necessary to consider the effect of inlet concentration on $\eta_{benzene}$ and Ey. Q was set at 2.28 m^3/h, T at 298 K and Rh at 60%. We investigated the $\eta_{benzene}$ and Ey at initial concentration varying from 100 to 3000 mg/m^3 under 80 and 135 W, which were presented in Fig. 5. With increasing inlet concentration of C_6H_6, $\eta_{benzene}$ decreases but Ey increases, which was in a good agreement to other's publishing [9]. As high as 20 g/kWh Ey was achieved for 2886 mg/m^3 C_6H_6 in this work.

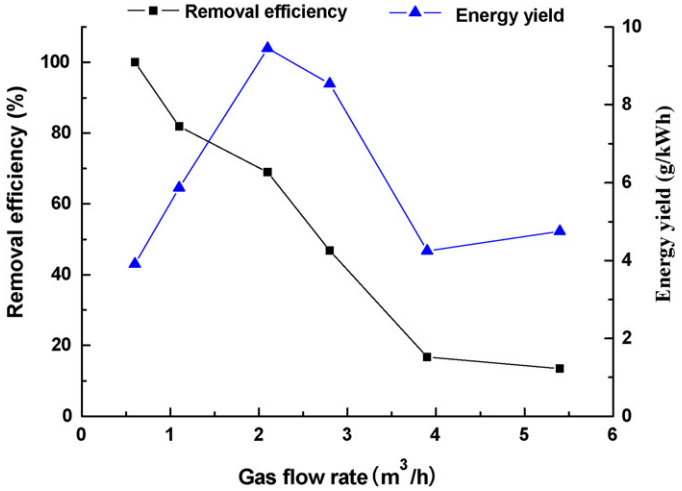

Fig. 4. Effect of Q on $\eta_{benzene}$ and Ey at 135 W (T = 289 K, Rh = 42%, C_{in} = 880 mg/m^3).

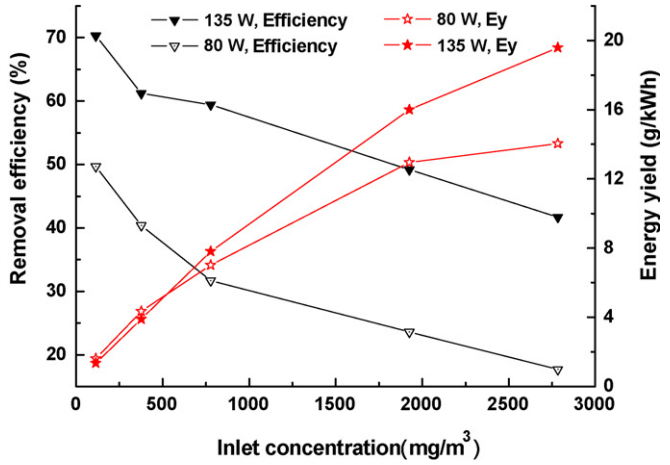

Fig. 5. Effect of C_{in} on $\eta_{benzene}$ and Ey at 80 W and 135 W (T = 298 K, Rh = 60%, Q = 2.28 m^3/h).

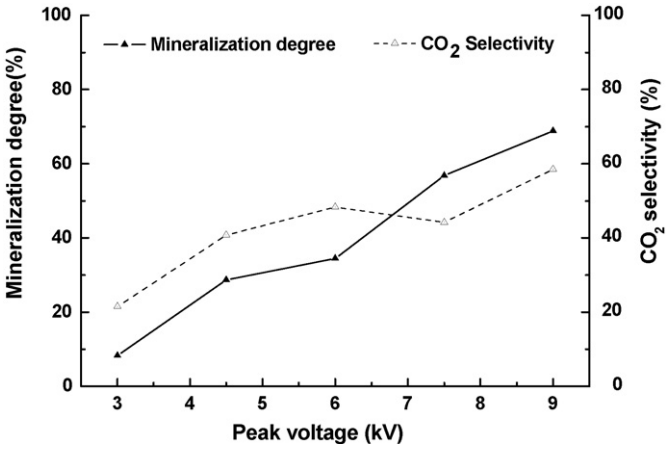

Fig. 6. Benzene mineralization degree and CO_2 selectivity as a function of peak voltage in DBD (T = 298 K, Rh = 56%, C_{in} = 1000 mg/m^3, Q = 2.10 m^3/h).

These findings also indicate that the energy efficiency for removing the same amount of C_6H_6 can be enhanced as the inlet benzene concentration is increased. Interestingly, in contrast to xylene removal [9] and carbon bisulfide (CS_2) removal [15], we found that the effect of inlet concentration on benzene removal in this work appears to be slighter. We cannot gain implicit answer at this stage, but the possible reasons for which have been speculated on the basis of two aspects: first, C_6H_6 molecule is very stable compared with CS_2 and xylene, only a series of radical reaction can destruct it. Consequently, though each C_6H_6 molecule in a lower concentration obtains more excited species, some C_6H_6 molecules still cannot be destructed, resulting in less increase in removal efficiency. Secondly, gas flow rate in this work is much higher (gas residence time is only 0.04–0.15 s), so some C_6H_6 molecule have not enough time to react with radicals, resulting in enhancing collision probability in low concentration C_6H_6 hard to represent in our work. Anyway, in order to improve energy efficiency, a relative high initial concentration would be desired.

In conclusion, lower flow rate, lower initial concentration, as well as higher input power contribute to higher $\eta_{benzene}$. Higher initial concentration, input power led to higher Ey. The effect of gas flow rate on Ey appears to be not linear and the highest Ey is up to 20 g/kWh in our experiment.

3.1.2. Degree of complete degradation

Practical application of DBD for pollutant decomposition must be considered based on not only removal efficiency but also safety of byproducts and degree of complete degradation. The desired final byproduct of carbon in VOCs structure is CO_2, since CO is still very toxic and also hard to be oxidized to CO_2 using plasma alone. We analyzed the mineralization degree and CO_2 selectivity after plasma reaction and the results are shown in Fig. 6. The experimental conditions are as follows: C_{in} of 1000 mg/m^3, Q of 2.10 m^3/h, T of 298 K, and Rh of 56%. As seen, both Md and S_{CO_2} increase as peak voltage increases. However, the variation of Md was most prominent for the C_6H_6 destruction with changing voltage because CO is relatively hard to be oxidized to CO_2 even in high voltage. The rise of high-energy electron amount in higher voltage contributes to the enhancement of mineralization degree, especially to stable pollutant molecule.

3.2. Experimental results in scale-up DBD system

Above results had demonstrated the effectiveness of the DBD system for C_6H_6 removal in a laboratory-scale DBD reactor and analyzed the influence factors. Consequently, we would like to test the efficiency in scale-up DBD system by simulating practical industrial exhausts under high-flow rate.

We carried out our experiment under one DBD system, two DBD systems in series, as well as three DBD systems in series. The total gas flow rate of 10 discharge tubes with parallel connection is 509 m^3/h. The inlet concentration of C_6H_6 varies from 2000 to 3300 mg/m^3, T of 298 K, and Rh of 50%. Notably, T and Rh would vary within a range of 3 K and 10%, respectively, due to weather condition. The results are listed in Tables 1 and 2.

As seen in Table 2, the highest $\eta_{benzene}$ is only 58.2% at 10.5 kV in one DBD system, but in two and three DBD systems in series, $\eta_{benzene}$ can reach 78.3 and 89.9% at 7.5 kV, respectively. Thus, we assure DBD system in series can enhance $\eta_{benzene}$. It is also not difficult to find that $\eta_{benzene}$ enhances significantly from one system to two systems in series, while only about 10% increase from two systems to three systems were found, so adding DBD number in series further does not increase $\eta_{benzene}$ greatly. Moreover, from one system to three systems, energy consumption tripling means that energy yield, which reflects the real efficiency of the system, actually decreases. Taking into account the energy yield and benzene conversion, we think one DBD system is more desirable.

Nevertheless, under our experimental condition, the outlet concentration of C_6H_6 after discharge is still high which is far beyond effluent standard of benzene, so it is necessary to consider combined plasma technology in actual application.

Unfortunately, after DBD run for a period of time, some brown residues were found to deposit on the inside wall of DBD, which changes dielectric constant of quartz tube and leads to thermal energy built up and finally mechanical failure

Table 1
Experimental results of benzene destruction in scale-up DBD system ($Q = 509\ m^3/h$, $T = 298\ K$, Rh = 50%)

Peak voltage (kV)	Input power (kW)	Inlet concentration (mg/m^3)	Outlet concentration (mg/m^3)	$\eta_{benzene}$ (%)
3	1.14	2078.2	1236.8	40.5
	1.12	2050.8	1201.4	41.4
	1.14	2341.2	1273.8	45.6
	1.14	2317.2	1271.5	45.1
6	1.61	2196.5	1146.1	47.8
	1.64	2579.3	1288.3	50.1
	1.63	2354.3	1226.0	47.9
	1.61	2291.5	1173.2	48.8
7.5	2.12	3172.0	1467.8	53.7
	2.19	2333.3	1066.7	54.3
	2.15	2263.3	1096.4	51.6
	2.18	2319.2	1064.1	54.1
9	2.82	3243.0	1408.3	56.6
	2.74	2266.7	1043.7	54.0
	2.79	2383.4	1084.7	54.5
	2.78	2523.3	1125.4	55.4
10.5	3.41	2325.2	955.65	58.9
	3.40	2503.2	1074.5	57.1
	3.41	2413.9	1029.4	57.4
	3.45	2389.3	973.7	59.2

of the dielectric. Therefore, after each run, air (without C_6H_6) was passed through DBD reactor at 6 kV for several minutes to remove the polymeric deposits.

3.3. Byproducts and mechanism analysis

3.3.1. Byproducts analysis

Most of the products in the effluent were CO and CO_2 and there were no products of partial oxidation by on-line GC analysis. Analyzing outlet gas collected in liquid nitrogen by FT-IR, we also did not find new strong bands. But we cannot jump to the conclusion that C_6H_6 removed was mineralized totally on the basis of these phenomena. Some aerosol particles were detected qualitatively in effluent via portable particles sizer (Dust-Sol, China).

In addition, in the inner wall of DBD tube, we did find a little brown residue, which can partially dissolve in dichloromethane (CH_2Cl_2) solvent but completely dissolve in methanol (CH_3OH) or acetone (C_3H_6O). The solid deposition also can be easily removed with a water wash. GC/MS analysis (Fig. 7) has shown that the main components of residues dissolved in acetone (chromatogram-grade) from benzene plasma are phenol, heptanoic acid, 2-nitro-phenol, hydroquinone, resorcinol, 3-nitro-phenol, 4-nitrocatechol, and 4-phenoxy-phenol. Sometimes, a small peak with a mass number appears in the chromatogram, but the corresponding mass spectrum quality is very poor. No matter what the DBD power or gas flow-rate is, phenol, hydroquinone and nitrophenol are always the main products in the deposition from C_6H_6 plasma. However, the relative yields vary with different conditions.

3.3.2. Discussions on reasons of formation of byproducts

3.3.2.1. Electron energy distribution in DBD reactor. The electrons energy distribution in DBD is in accordance with Maxwell function and the percentage of electrons whose energy value is equal to ε can be expressed as Eq. (1) [17].

$$f(\varepsilon) = 2.07(\bar{\varepsilon})^{-3/2}\varepsilon^{1/2}e^{-1.5\varepsilon/\bar{\varepsilon}} \quad (1)$$

Here, $f(\varepsilon)$ represents the percentage, $\bar{\varepsilon}$ denotes average energy of electrons in DBD system.

Bai and coworkers [18] had calculated that average energy ($\bar{\varepsilon}$) is equal to 5.0 eV in DBD system according to its discharge

Table 2
Experimental results of benzene destruction in DBD systems in series ($Q = 509\ m^3/h$, $T = 298\ K$, Rh = 50%)

Peak voltage (kV)	Inlet concentration (mg/m^3)	Input power (kW)			Removal efficiency (%)		
		One[a]	Two[b]	Three[c]	One[a]	Two[b]	Three[c]
6	2355	1.63	3.26	4.89	48.7	73.7	86.5
7.5	2522	2.23	4.46	6.69	53.4	78.3	89.9
9	2604	2.82	5.64	8.46	55.1	79.8	90.9
10.5	2408	3.42	6.84	10.26	58.2	82.5	92.7

[a] One DBD system.
[b] Two DBD system in series.
[c] Three DBD system in series.

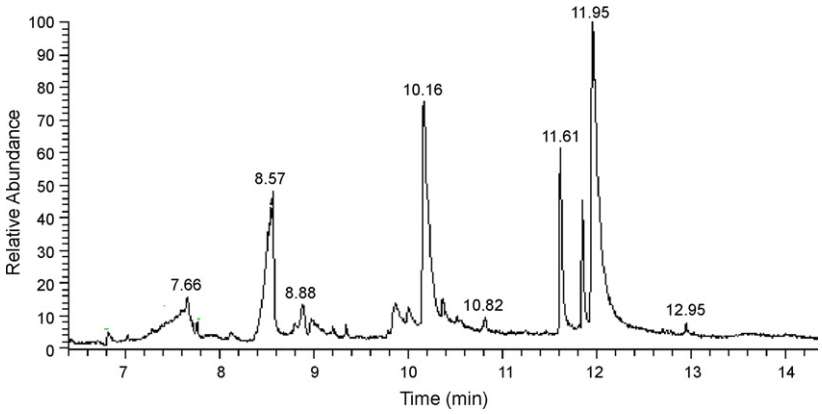

Fig. 7. GC–MS spectrum of solid residues of benzene destruction in DBD (80 W, 20 kHz) (7.66: phenol; 8.57: heptanoic acid; 8.88: 2-nitro-phenol; 10.16: hydroquinone; 10.82: resorcinol; 11.61: 3-nitro-phenol; 11.95: 4-nitrocatechol; 12.95: 4-phenoxy-phenol).

parameters. So, we can obtain Eq. (2) when $\bar{\varepsilon} = 5.0$ was placed in Eq. (1).

$$f(\varepsilon) = 2.07 \times (5.0)^{-3/2}\varepsilon^{1/2}e^{-0.3\varepsilon} = 0.185\varepsilon^{1/2}e^{-0.3\varepsilon} \quad (2)$$

By integral operation on Eq. (2) with bottom line of "a" value and top line of "$+\infty$" value, we can gain the percentage of electron ($\rho_{E(a)}$) whose energy value is higher than "a" value.

$$\rho_{E(a)} = \int_a^{+\infty} f(\varepsilon)\,d\varepsilon = \int_a^{+\infty} 0.185\varepsilon^{1/2}e^{-0.3\varepsilon}\,d\varepsilon \quad (3)$$

By a series of mathematical operations and equation counterchanges to Eqs. (3) and (4) can be obtained.

$$\rho_{E(a)} = \int_a^{+\infty} f(\varepsilon)\,d\varepsilon = 0.185 \times [\sqrt{0.3a}/2e^{-0.3a} + 0.3^{-3/2}e^{-0.3a}(\sqrt{0.3a} + \sqrt{\pi}/2)]. \quad (4)$$

3.3.2.2. The mechanism discussion of C_6H_6 destruction in DBD. It is well known that C_6H_6 molecule is very stable. Bond energy of C=C in C_6H_6 molecule is 5.4 eV, so only high-energy electron beyond 5.4 eV can make C_6H_6 molecule ring-cleavage dissociation. According to Eq. (4), we can calculate that the percentage of electron higher than 5.4 eV is about 45.8%, thereby only less than half benzene molecules can possess ring-cleavage dissociation. However, almost 90% C_6H_6 was removed in DBD based on previous experimental results [19]. Hence, there must existed many complicated reactions in DBD which led to C_6H_6 destruction except for direct dissociation of C_6H_6 molecule by high-energy electrons impact.

Even for small molecules, the reaction mechanisms for pollutant destruction can be complicated. Complex molecules often undergo a series of intermediate reactions before they are completely destructed in plasma. Since the mechanism of C_6H_6 destruction in DBD is unclear up to now, we would offer relative overall mechanism for C_6H_6 destruction by referring to some related publications [20–25] and our experimental results in this work.

First, the high-energy electron attacks oxygen to generate O atoms due to its relative higher concentration as background gas and low bond energy (5.1 eV of O–O bond). Furthermore, high-energy electron attacks C_6H_6 molecule to generate phenyl ($C_6H_5^{\bullet}$) attributed to C–H bond breakage [3].

$$O_2 \xrightarrow{e} O + O \quad (5)$$

$$C_6H_6 \xrightarrow{e} C_6H_5^{\bullet} + H^{\bullet} \quad (6)$$

Further, O atom behaves as a strong oxidant to produce other oxidation products and radicals such as O_3, $HO_2^{\bullet}$ and $^{\bullet}OH$ by extracting hydrogen atoms or other reactions [20–22].

$$O + O_2 \rightarrow O_3 \quad (7)$$

$$O + H^{\bullet} \rightarrow OH^{\bullet} \quad (8)$$

$$O + OH^{\bullet} \rightarrow H^{\bullet} + O_2$$
$$k_1 = 3.3 \times 10^{-11}\,cm^3\,molecule^{-1}\,s^{-1} \quad (9)$$

$$O + {}^{\bullet}HO_2 \rightarrow OH^{\bullet} + O_2$$
$$k_2 = 5.4 \times 10^{-11}\,cm^3\,molecule^{-1}\,s^{-1} \quad (10)$$

$$^{\bullet}OH + {}^{\bullet}OH \rightarrow H_2O + O,$$
$$k_3 = 1.8 \times 10^{-12}\,cm^3\,molecule^{-1}\,s^{-1} \quad (11)$$

These radical species ($^{\bullet}H$, $^{\bullet}HO_2$, $^{\bullet}OH$) react with $C_6H_5^{\bullet}$, and C_6H_6 to form C_6H_5OH, $C_6H_5O^{\bullet}$ or other oxidation products (CO, CO_2, etc.) by breaking the aromatic structure. Relative reactions and rate constants came from some other references [23–25] and were listed below.

$$O + C_6H_6 \rightarrow C_6H_5OH \quad (12)$$

$$C_6H_5^{\bullet} + O_2 \rightarrow C_6H_5OO^{\bullet} \rightarrow C_6H_5O^{\bullet} + O,$$
$$k_4 = 1.97 \times 10^{-12}\,cm^3\,molecule^{-1}\,s^{-1} \quad (13)$$

Table 3
TCP estimation of benzene destruction in DBD ($Q = 509\ m^3/h$, $T = 298\ K$, Rh = 50%, and input power is listed in Table 2)

Voltage (kV)	C_{in} (mg/m^3)	One[a]		Two[b]		Three[c]	
		η (%)	TCP ($/m^3)	η (%)	TCP ($/m^3)	η (%)	TCP ($/m^3)
6	2355	48.7	0.00024	73.7	0.00048	86.5	0.00072
7.5	2522	53.4	0.00034	78.3	0.00068	89.9	0.00102
9	2604	55.1	0.00043	79.8	0.00086	90.9	0.00129
10.5	2408	58.2	0.00052	82.5	0.00104	92.7	0.00156

[a] One DBD system.
[b] Two DBD system in series.
[c] Three DBD system in series.

Table 4
Detailed material and reaction condition of plasma reactors

Reactor	Material	Packing	Q (L/min)	Inlet concentration (mg/m^3)	Peak voltage (kV)
Pulse corona [27]	Quartz	–[a]	0.2–3	522	–[a]
Glow discharge [28]	–[a]	–[a]	0.1	1031	0.47
Surface discharge [27]	Quartz	–[a]	0.2–3	522	–[a]
MnO_2-DBD [29]	Glass	MnO_2	0.5	366	–[a]
Ag/TiO_2-plasma [27]	Pyrex	Ag/TiO_2	0.2–3	522	–[a]
This work (laboratory)	Quartz	–[a]	35	880	9
This work (scale-up)	Quartz		8483	2604	9

[a] No original date.

$$C_6H_5^{\bullet} + OH^{\bullet} \rightarrow C_6H_5\text{–OH adduct} \rightarrow C_6H_5OH,\quad k_5 = 1.3 \times 10^{-12}\ cm^3\ molecule^{-1}\ s^{-1} \quad (14)$$

$$C_6H_5O^{\bullet} + H^{\bullet} \rightarrow C_6H_5OH \quad (15)$$

$$C_6H_5O^{\bullet} + HO_2^{\bullet} \rightarrow C_6H_5OH + O_2,\quad k_6 = 1.0 \times 10^{-12}\ cm^3\ molecule^{-1}\ s^{-1} \quad (16)$$

$$C_6H_6 + OH^{\bullet} \rightarrow C_6H_6\text{–OH adduct},\quad k_7 = (1.1 - 1.4) \times 10^{-13}\ cm^3\ molecule^{-1}\ s^{-1} \quad (17)$$

$$C_6H_6\text{–OH adduct} + O_2 \rightarrow C_6H_6\text{–}OHO_2\text{ adduct},\quad k_8 = 3.3 \times 10^{8}\ L\ mol^{-1}\ s^{-1} \quad (18)$$

$$C_6H_6 + H^{\bullet} \rightarrow C_6H_6\text{–H adduct},\quad k_9 = (5.3 \pm 1.0) \times 10^{8}\ L\ mol^{-1}\ s^{-1} \quad (19)$$

$$O + C_6H_6, C_6H_5OH \rightarrow \text{other oxidation products (CO, } CO_2\text{, etc.)} \quad (20)$$

Meanwhile, a comparative amount of nitrophenol was detected in solid residues, which indicates that part N≡N bonds are broken in spite of its higher bond energy (9.7 eV) into N atoms. It was suggested that the NO_2 from reaction of N-atom with O_2 resulted in nitrophenol occurring in products.

$$N_2 \xrightarrow{e} N + N \quad (21)$$

$$N + O_2 \rightarrow NO_2 \quad (22)$$

$$C_6H_5OH \xrightarrow{e} {}^{\bullet}C_6H_4OH + {}^{\bullet}H \quad (23)$$

$$C_6H_4OH^{\bullet} + NO_2 \rightarrow C_6H_4OH\text{–}NO_2 \rightarrow C_6H_4OHNO_2 \quad (24)$$

Table 5
Comparison of benzene removal between various plasma reactors

Reactor	$\eta_{benzene}$ (%)	SED (J/L)	k_E (L/J)	Ey (g/kWh)
Pulse corona [27]	25	264	$2.2 \pm 0.2 \times 10^{-3}$	1.78[b]
Glow discharge [28]	–[a]	3370–6030	–[a]	0.53–0.87
Surface discharge [27]	36.9	288	$2.5 \pm 0.2 \times 10^{-3}$	2.41[b]
MnO_2-DBD [29]	55	360	–[a]	2.01[b]
Ag/TiO_2-plasma [27]	89.1	391	$5.0 \pm 0.2 \times 10^{-3}$	4.28[b]
This work (laboratory)	69.0	232	$4.6 \pm 0.2 \times 10^{-3}$	9.45
This work (scale-up)	55.1	11.1	–[a]	465.3

[a] No original date.
[b] Calculated from original date.

3.4. Feasibility study

3.4.1. Treatment cost estimation

According to the data in Table 2, we calculated treatment cost per unit volume (TCP ($/m^3) = PR/Q; R is power rate ($/kWh)), which was listed in Table 3. In our experiment, Q is equal to 509 m^3/h and R is 0.61 RMB/kWh in Shanghai, corresponding to 0.077 $/kWh. The data in Table 3 suggest that TCP rises with the increase of peak voltage. DBD system in series can improve the removal efficiency at the cost of increasing treatment cost. For instance, TCP rise to three times when $\eta_{benzene}$ increased from 48.7% in one DBD system to 86.5% in three systems at 6 kV. Two main conclusions were obtained with a view to treatment cost: first, we should select lower voltage for benzene removal with DBD in order to lower TCP; secondly, the TCP of C_6H_6 with DBD is acceptable and C_6H_6 removal with DBD is feasible.

3.4.2. Comparison with other plasmas

To assess a plasma technology for pollutant treatment, removal efficiency (η) and energy efficiency were widely used. Energy efficiency has several expression styles including specific energy density (SED (J/L) = 3.6 P/Q), energy yield (Ey, g/kWh), and energy constant (k_E, L/J). k_E can be fairly well described by first-order kinetics as a function of SED and $\eta(-\ln(1-\eta) = k_E$ SED) [26]. In this paper, we attempted to get a performance comparison between this work and others' works in terms of η, SED, k_E and Ey. Larger k_E and Ey indicates higher capability in pollutants decomposition with plasmas, while it is reverse to SED value [27]. However, η, Ey, SED and k_E varies with many factors, so we present corresponding conditions including dielectric materials and reaction conditions (Table 4).

Table 5 summarizes $\eta_{benzene}$, SED, Ey and k_E for benzene removal with various non-thermal plasma technologies. As shown in Table 5, the order of k_E was Ag/TiO_2-plasma > this work (laboratory) > surface discharge ≈ pulse corona; SED increases in the order of this work (scale-up) < this work (laboratory) < pulse corona < surface discharge < MnO_2-DBD < Ag/TiO_2-plasma < Glow discharge. Accordingly, the order of Ey is: this work (scale-up) > this work (laboratory) > Ag/TiO_2-plasma > surface discharge > MnO_2-DBD > pulse corona > glow discharge. Lower SED and higher k_E and Ey in this work indicated that DBD in this work had a higher energy efficiency compared with other plasmas.

3.4.3. Problems existed in DBD treatment

By above analysis, we can see that DBD is a very effective approach to treat gas stream containing C_6H_6. It has many advantages compared with other technologies. Its treatment cost per unit volume is also acceptable. Even though, there still some problems including aerosol particles in effluent and solid residues in the wall of tube need to be considered. Although the addition of O_2 helps decompose C_6H_6 and effectively suppressed aerosol particles formation in plasma [30] and air (without C_6H_6) was passed through DBD reactor several minutes to remove solid residues in the wall of tube, they cannot be removed completely because the formation and growth pathway of them is still poorly understood. These issues are not well understood and solved at the present time, so they deserve our further investigation in future.

4. Conclusion

This study presents detailed description of C_6H_6 removal with DBD including operation parameters, byproducts and reaction pathways discussion, and feasibility analysis. Input power, gas flow rate, and initial concentration of C_6H_6 have great effects on $\eta_{benzene}$ and Ey. The highest Ey can reach 20 g/kWh in our experiment. The reaction mechanisms of C_6H_6 in DBD are very complicated due to the attendance of radical species produced in discharge process. DBD system in series can enhance $\eta_{benzene}$ to a large extent. The feasibility study shows that DBD has high superiority in contrast to other technologies, while there are still some problems including aerosol particles in effluent and solid residues in the wall of tube. These issues must be well solved before actual commercial application.

References

[1] H.M. Lee, M.B. Chang, Gas-phase removal of acetaldehyde via packed-bed dielectric barrier discharge reactor, Plasma Chem. Plasma Process. 21 (2001) 329–343.
[2] H.X. Ding, A.M. Zhu, F.G. Lu, Y. Xu, J. Zhang, X.F. Yang, Low-temperature plasma-catalytic oxidation of formaldehyde in atmospheric pressure gas streams, J. Phys. D: Appl. Phys. 39 (2006) 3603–3608.
[3] H. Sekiguchi, M. Ando, H. Kojima, Study of hydroxylation of benzene and toluene using micro-DBD plasma reactor, J. Phys. D: Appl. Phys. 38 (2005) 1722–1727.
[4] D. Ascenzi, P. Franceschi, G. Guella, P. Tosi, Phenol production in benzene/air plasmas at atmospheric pressure: role of radical and ionic routes, J. Phys. Chem. A. 110 (2006) 7841–7847.
[5] H.H. Kim, A. Ogata, S. Futamura, Effect of different catalysts on the decomposition of VOCs using flow-type plasma-driven catalysis, IEEE Trans. Plasma. Sci. 34 (2006) 984–995.
[6] A. Ogata, K. Miyamae, K. Mizuno, S. Kushiyama, M. Tezuka, Decomposition of benzene in air in a plasma reactor: effect of reactor type and operating conditions, Plasma Chem. Plasma Process. 22 (2002) 537–552.
[7] Y.F. Guo, D.Q. Ye, K.F. Chen, Toluene removal characteristics by a superimposed wire-plate dielectric barrier discharge plasma reactor, J. Environ. Sci. 18 (2006) 276–280.
[8] Ch. Subrahmanyam, A. Renken, L. Kiwi-Minsker, Catalytic abatement of volatile organic compounds assisted by non-thermal plasma. Part II. Optimized catalytic electrode and operating conditions, Appl. Catal. B: Environ. 65 (2006) 150–156.
[9] H.M. Lee, M.B. Chang, Abatement of gas-phase *p*-xylene via dielectric barrier discharges, Plasma Chem. Plasma Process. 23 (2003) 541–558.
[10] C.L. Chang, H. Bai, S.J. Lu, Destruction of styrene in an air stream by packed dielectric barrier discharge reactors, Plasma Chem. Plasma Process. 25 (2005) 641–657.
[11] G.K. Anderson, H. Snyder, J. Coogan, Oxidation of styrene in a silent discharge plasma, Plasma Chem. Plasma Process. 19 (1999) 131–151.
[12] S. Tanabe, Oligomerization and carbon dioxide reforming of methane in a dielectric-barrier discharge-plasma system, J. Jpn. Pet. Assoc. 42 (1999) 383–391.
[13] J. Hou, X.N. Liu, H.Q. Hou, Cold plasma technology and its application to treatment organic industrial waste gases, Shanghai Environ. Sci. 18 (1999) 151–153.
[14] B. Lu, X. Zhang, X. Yu, T. Feng, S. Yao, Catalytic oxidation of benzene using DBD corona discharges, J. Hazard. Mater. B 137 (2006) 633–637.

[15] H.J. Fang, H.Q. Hou, L.Y. Xia, X.H. Shu, R.X. Zhang, A combined plasma photolysis (CPP) method for removal of CS_2 from gas streams at atmospheric pressure, Chemosphere 69 (2007) 1734–1739.
[16] G.Y. Zheng, J.M. Jiang, Y.P. Wu, R.X. Zhang, H.Q. Hou, The mutual conversion of CO_2 and CO in dielectric barrier discharge (DBD), Plasma Chem. Plasma Process. 23 (2003) 59–68.
[17] Plasma Chemistry and Processing (in Chinese), Publishing House of the University of Science and Technology of China, Hefei, China, 1993.
[18] X.Y. Bai, Z.T. Zhang, M.D. Zhang, Q.Y. Zhu, Nonequilibrium plasma chemistry at higher pressure and its applications, Physics 29 (2000) 406–410.
[19] J.M. Jiang, J. Hou, G.Y. Zhen, H.Q. Hou, The decomposition of benzene and xylene under normal atmospheric pressure by dielectric barrier discharge, China Environ. Sci. (in Chinese) 21 (2001) 531–534.
[20] T. Berndt, O. Böge, H. Herrmann, On the formation of benzene oxide/oxepin in the gas-phase reaction of OH radicals with benzene, Chem. Phys. Lett. 314 (1999) 435–442.
[21] K.J. Hsu, J.L. Durant, F. Kaufman, Rate constants for atomic hydrogen + oxygen + M at 298 K for M = helium, nitrogen, and water, J. Phys. Chem. 91 (1987) 1895–1899.
[22] T. Yu, M.C. Lin, Kinetics of phenyl radical reactions studied by the cavity-ring-down method, J. Am. Chem. Soc. 115 (1993) 4371–4372.
[23] D. Ascenzi, P. Franceschi, G. Guella, P. Tosi, Phenol production in benzene/air plasmas at atmospheric pressure. Role of radical and ionic routes, J. Phys. Chem. A 110 (2006) 7841–7847.
[24] M. Roder, L. Wojharovits, G. Foldiak, Pulse radiolysis of aqueous solutions of aromatic hydrocarbons in the presence of oxygen, Radiat. Phys. Chem. 36 (1990) 175–176.
[25] B.D. Michael, E.J. Hart, Rate constants of hydrated electron, hydrogen atom, and hydroxyl radical reactions with benzene 1, 3-cyclohexadiene 1, 4-cyclohexadiene, and cyclohexene, J. Phys. Chem. 74 (1970) 2878–2884.
[26] H.H. Kima, G. Prietob, K. Takashima, S. Katsura, A. Mizuno, Performance evaluation of discharge plasma process for gaseous pollutant removal, J. Electrostat. 55 (2002) 25–41.
[27] H.H. Kim, H. Kobara, A. Ogata, S. Futamura, Comparative assessment of different nonthermal plasma reactors on energy efficiency and aerosol formation from the decomposition of gas-phase benzene, IEEE Trans. Ind. Appl. 41 (2005) 206–214.
[28] C.Q. Jiang, A. Aleam, H. Mohamed, H. Robert, Stark, H. James, H. Karl, Removal of volatile organic compounds in atmospheric pressure air by means of direct current glow discharges, IEEE Trans. Plasma. Sci. 33 (2005) 1416–1425.
[29] S. Futamura, H. Einaga, H. Kabashima, L.Y. Hwan, Synergistic effect of silent discharge plasma and catalysts on benzene decomposition, Catal. Today 89 (2004) 89–97.
[30] S.I. Shih, T.C. Lin, M. Shih, Decomposition of benzene in the RF plasma environment. Part II. Formation of polycyclic aromatic hydrocarbons, J. Hazard. Mater. B 117 (2005) 149–159.